Experimental Study of Shape Transitions and Energy Scaling in Thin Non-Euclidean Plates

Yael Klein, Shankar Venkataramani, and Eran Sharon

Phys. Rev. Lett. **106**, 118303 — Published 14 March 2011

DOI: 10.1103/PhysRevLett.106.118303

An Experimental Study of Shape Transitions and Energy Scaling in Thin Non-Euclidean Plates

Yael Klein, Shankar Venkataramani and Eran Sharon

Abstract

We present the first quantitative measurements of shape and energy variation in non-Euclidean plates. Using environmentally responsive gel, we construct non-Euclidean discs of constant imposed Gaussian curvature, K_{tar}. We vary the discs thickness, t_0, and measure the dependence of configurations, surface curvature and energy content on t_0. For $K_{tar}<0$ configurations are of a single wavy mode, and undergo a set of bifurcations that leads to their refinement with decreasing thickness. This leads to sharp increase in the amount of surface bending as $t_0 \rightarrow 0$,and toa slow decay of both bending and stretching energies. Both vary like t_0^2, compared with t_0^3 of the bending energy in discs with $K_{tar}>0$.

Recently there is an increasing interest in the construction of structures that are capable of inducible large shape transformations. An interesting group of such bodies is that of non-Euclidean elastic plates. These structures can be generated by irreversible deformations of originally flat plates [1, 2], the non-uniform swelling or shrinkage of plates [3], or from non-uniform, yet lateral, growth of natural sheets [4]. Though intrinsically uniform across their thickness (thus called plates) the intrinsic two-dimensional (2D) geometry of the mid surface of these sheets is non-Euclidean. The laterally non-uniform expansion/shrinkage of the sheet specifies a 2D "target metric" tensor, g_{tar}, with non vanishing Gaussian curvature [5], K_{tar} (thus the term non-Euclidean) (see [6], [7]). As a result the plates buckle into three-dimensional (3D) configurations that are consistent with the target metric. Small changes in the target metric can lead to qualitative and substantial quantitative differences in the selected configurations. This sensitivity is of potential interest for different applicative fields, such as bio-mechanics and soft robotic, in particular when the plates are generated with environmentally responsive materials, as in [3].

Different theoretical approaches have been used in order to study the configurations adopted by non-Euclidean plates, including 3D [8] and 2D [9] numerical simulations, purely geometrical analysis [10] and an analytical study of different approximations of the problem [11,12].

Recently we have used environmentally responsive gels to construct non-Euclidean elastic discs with an inducible, axi-symmetric, prescribed target metric [3]. When the imposed metric was hyperbolic ($K_{tar}<0$), the discs adopted multi wave configurations, breaking the axial symmetry. The basic shape selection of such hyperbolic plates is still not well understood. Specifically, what determines the wavelength cascade? Does the thickness only provide a cutoff scale, or is there an explicit dependence of wavelength on t, which can lead to singular behavior in the limit $t\rightarrow 0$?

One can identify three quantities with length dimensions that can play a role in determining wavelength selection: The sheet thickness, t, the disc radius, R, and a geometrical length, $L\sim K_{tar}^{-1/2}$.Which combination of the above determines the waviness? In previously studied cases [9,2] K_{tar} varied across the disc, leading to L=L(**r**), with no fixed length scale. Having a constant value of L across the discs will result in three length *scales,* enabling isolation of the affect of each of these scales on the wavelength.

In this work we constructed gel discs with a prescribe constant Gaussian curvature, $K_{tar}=Const$, resulting in L being constant across the discs. We used a fixed K_{tar} and radius R for all discs, varying only the initial sheet thickness t_0. This enables us to study both the scale dependence and the behavior as $t_0\rightarrow 0$. Three main observations are made for all hyperbolic ($K_{tar}<0$) discs: Wavy patterns are of a *single* (azimuthal) mode (no multi-wave configurations were observed); There is an explicit dependence of wavelength on plate thickness; The amount of surface bending strongly increases with decreasing thickness, leading to a "slow" decay of bending energy, $E_b\sim t_0^2$. For $K_{tar}>0$, the amount of surface bending is bounded, and the energy decays as in "regular" buckling, $E_b\sim t_0^3$.

Axially symmetric N-IsoproPylAcrylamide (NIPA) hydro gel discs were prepared as in [3], with the addition of explicit control of the radial dependence of the NIPA concentration, C(r). Above $33C^0$ a radially dependent (though locally isotropic) shrinkage of distances on the discs, $\eta(r)=\eta(C(r))$, occurs, with η ranging from 0.4 to 0.9 within each disc. This allows using C(r) as a knob, to program g_{tar} (and thus K_{tar}) on the discs. In the current work we have constructed NIPA profiles C(r) that result in a constant Gaussian curvature $|K_{tar}|= 0.0011$ mm^{-2} on *all* the discs. The corresponding $\eta(C(r))$ yield first fundamental forms: $dl^2 = d\rho^2 + K_{tar}^{-1}\sin^2\left(\rho\sqrt{K_{tar}}\right)d\theta^2$, for $K_{tar}>0$,

and $dl^2 = d\rho^2 - K_{tar}^{-1}\sinh^2\left(\rho\sqrt{-K_{tar}}\right)d\theta^2$, for $K_{tar}<0$. Here θ is the azimuthal coordinate and $\rho = \int_0^r \eta(r')dr'$ is the radius on the surface after shrinkage.

Disc radii were fixed at $\rho_{max} \equiv R=28$ (+/- 1) mm. discs' thickness (prior to shrinkage) t_0 was 0.1-1.5 mm. The discs were heated and dried as in [3] and their topography was measured optically with horizontal and vertical resolutions of 25μm and 5μm, respectively. A semi geodesic (see [5])polar coordinate system, (ρ, θ) was defined on the measured surfaces, and the local Gaussian ($K(\rho, \theta)$) and mean ($H(\rho, \theta)$) curvatures were computed for each disc. Direct thickness measurements on selected discs show that, to a good approximation, the local thickness following shrinkage is given by $t(r)=t_0\eta(r)$.

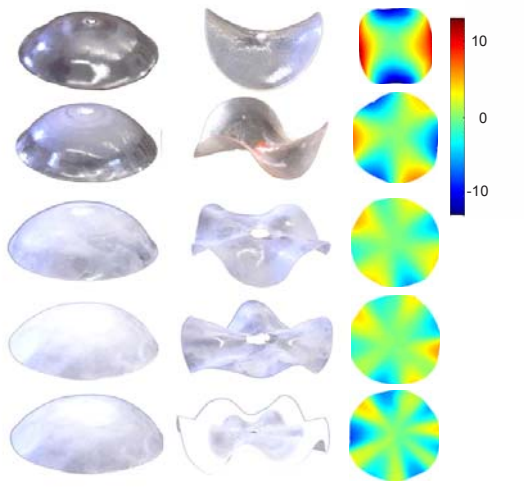

Figure1: Variation of configurations with thickness. Discs of K_{tar}= 0.0011 mm^{-2} (left) and K_{tar}= -0.0011 mm^{-2} (middle and right) of various initial thicknesses (t_0=0.75, 0.6, 0.25, 0.19 and 0.125 mm top to bottom). For $K_{tar}>0$ the discs keep the same basic shape, a hemisphere, with minor variations, along the edge. The discs of $K_{tar}<0$ undergo a set of bifurcations, in which the number of nodes, *n*, increases with decreasing thickness. Surface amplitude of hyperbolic discs (Right) shows that each configuration consists of a *single* wavy mode (The color bar, in mm, is common to all figures).

For varying thickness, two qualitatively different behaviors are observed (Fig. 1): All discs of $K_{tar}>0$ attain a dome-like configuration. On the other hand, the shape of the discs of $K_{tar}<0$ strongly depends on the thickness. Thick discs (Fig.1 top middle pane) attain a single saddle configuration.As t_0 decreases this configuration is replaced by multi-node wavy configurations. Unlike previously studied sheets [1, 8, 9, 2] all observed

configurations contain only a *single* wave mode . Multi scale patterns are, thus, not a must in hyperbolic sheets.

A configuration of n nodes can be written as $z(r,\theta)= A_n(r)\Phi(n\theta)$, where Φ is an unspecified normalized function, and is characterized by the number of nodes, n, and the amplitude profile, $A_n(r)$. Plotting n verses the thickness, t_0, shows a series of *shape transformations*, namely a refinement of the wavelength with decreasing thickness, where the number of nodes is roughly proportional to $t^{-0.5}$ (Fig. 2a). Surface measurements show that $A_n(r)$increase convexly towards the margins(Fig.2b). This is expected for the observed single mode configurations, since in these hyperbolic discs the perimeter increases faster than linearly with ρ. The increase in *n* is accompanied by a simultaneous decrease in $A_n(r)$, while the rescaled profiles, $nA_n(r)$ collapse onto a single curve (Inset of Fig. 2b). A rough estimation of the typical azimuthal and radial curvatures of the observed profiles gives $\kappa_\theta \sim \frac{A_n n^2}{r^2}$ and $\kappa_\rho \sim (A_n)_{rr}$ respectively. Assuming that the observed configurations roughly conform with the target metric, $K \sim K_{tar}$ (Where $K = \kappa_\theta \kappa_\rho$), and thus $\frac{(A_n)_{rr} A_n n^2}{r^2} \approx -K_{tar} = const$. This leads to the estimation: $A_n(r) \approx \sqrt{|K_{tar}|}\frac{r^2}{n}$, which is consistent with the scaled data (solid line in the inset of Fig. 2b). Thus, *on average*, all configurations well approximate the target metric.

We turn our attention to the bending content of the discs, ***B(r)***$\sim 4H(r)^2-K(r)$., whichis related to the total bending energy of a configuration by: $E_b \sim \iint d^2\mathbf{r} t^3 \mathbf{B(r)}$, and is not uniquely determined by the metric[5]. The spatial average of ***B(r)***, <***B***>, for discs of various thickness is shown inFig. 3 a. For $K_{tar}>0$, the bending content slightly increases with decreasing thickness, stabilizing and approaching a constant value, of the order of the prescribed K_{tar} ,. On the other hand, discs of negative curvature bend more and more with decreasing thickness. For the thinnest discs generated, of $t_0=100\ \mu m$, the average bending content is an order of magnitude larger than $|K|$. This increase in <***B***> at small thickness is a direct result of the refinement process: The mean curvature attains values on the order of $H \sim \kappa_\rho + \kappa_\theta = \sqrt{-K_{tar}}\left(n + \frac{1}{n}\right)$ leading to the relation <***B***>$\sim n^2$ for large n. As $n \sim t_0^{-0.5}$ (Fig. 1), we expect to have <***B***>$\sim t_0^{-1}$, which implies a divergence of the bending content in the limit $t \to 0$.

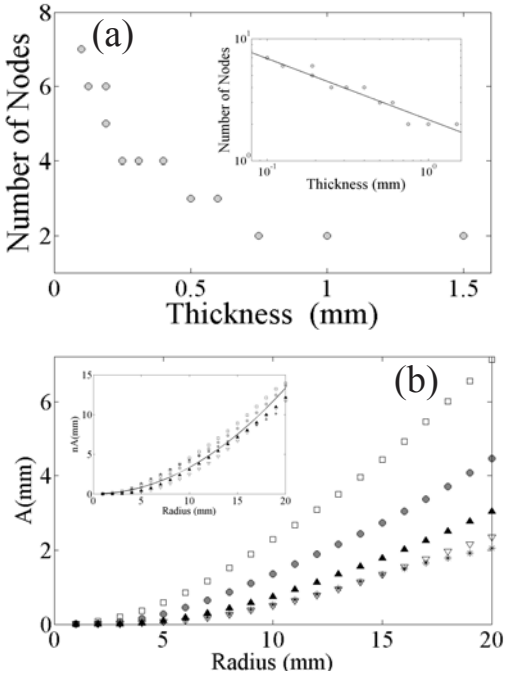

Figure2: (a) The number of nodes, *n*, as a function of sheet thickness for discs of K_{tar}= -0.0011 mm^{-2}. A log-log plot (inset) shows that the data are well described by $n \sim t_0^{-0.5}$ (solid line). (b) The amplitude of the waviness, A, as a function of radius on the buckled disc, for configurations with different number of nodes, *n= 2* to *6* (open squares down to stars). Inset, Multiplying A(r) by *n* leads to data convergence that is well described by $nA_n(r) = \sqrt{|K_{tar}|}r^2$ (solid line).

Indeed, $\langle \boldsymbol{B} \rangle \sim t_0^{-1}$ (inset of Fig 3a) and persists to the smallest thickness, without any saturation. We thus believe that refinement of the wavy configurations, together with the increase in the bending content, would persist to thickness significantly smaller than 0.1 mm.

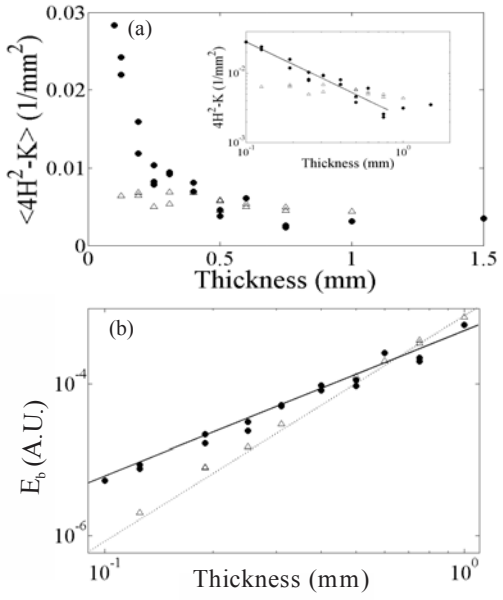

Figure 3: Scaling of curvature and energy. (a) The average bending content, <***B***>, as a function of sheet thickness. For $K_{tar}<0$ (solid circles)<***B***> increases sharply with decreasing thickness to values an order of magnitude larger than $|K|$. For $K_{tar}>0$, <***B***> is "saturated" at small thickness. Plotting the same data on a log-log scale (inset) shows that for $K_{tar}<0$, $\langle B \rangle \sim t_0^{-1}$ (solid line). (b) The total bending energy in a disc versus thickness. In the discs of $K_{tar}>0$ (open triangles) the energy decays like $t_0^{3\pm0.1}$ (dotted line), while for $K_{tar}<0$ (solid circles) the bending energy scales like $t_0^{1.9\pm0.1}$ (solid line).

The different dependence of bending content on t in the elliptic and hyperbolic discs, leads to different decay of the E_b with decreasing thickness (Fig. 3 b). For $K_{tar}>0$, the bending energy decays as t_0^3, while for $K_{tar}<0$, it decays much more slowly, as $t_0^{1.9\pm0.1}$. This suggests that the refinement is a stretching driven process. The sharp increase in bending content must be compensated by a simultaneous (and fast enough) decrease in stretching content with n.

The stretching energy is given by $E_s \sim \iint dr^2 t(\boldsymbol{r}) \boldsymbol{S}(\boldsymbol{r})$. ***S(r)***, the stretching content, is expressed by local differences between the actual metric of the disc, g (ρ,θ), and the target metric [13]. In our system, these differences are too small to be measured directly. However, measurements of the local Gaussian curvature can provide information about the variation of stretching content with thickness. Using the connection between a metric of a surface and its Gaussian curvature (Gauss Theorema Egregium), one can formally express ***S(r)*** in terms of the differences between the actual and target Gaussian curvatures; $\Delta K(\rho,\theta) \equiv K(\rho,\theta) - K_{tar}$. Configurations in which $\Delta K=0$ everywhere have zero stretching, while for $\Delta K \neq 0$, which fluctuates around zero over a typical scale L, the stretching content is of order $\Delta K^2 L^4$. As K_{tar}=const= -0.0011 mm^{-2}, $\Delta K(\rho,\theta) = K(\rho,\theta)+0.0011$, regardless of the position on the disc[14]. The spatially averaged value of the measured Gaussian curvature, <K>, roughly equals K_{tar} (i.e. $\langle \Delta K \rangle \approx 0$) independently of t_0 (Fig.4). This is an additional indication that all configurations are close to embeddings of the target metric. This, however, does not imply that the *local* value of K equals K_{tar}. We find that ΔK oscillates azimuthally, in correlation with the surfaces' waviness (see [3]). This implies that as the number of nodes, *n,* increases, the oscillation scales decrease as $L \sim 1/n$. The stretching content within a disc of n nodes is, therefore proportional to $\frac{\langle \Delta K^2 \rangle}{n^4}$. Using this connection we find that the stretching content of the hyperbolic discs varies linearly with the thickness (Fig. 4). This implies that the stretching energy scales as t_0^2 , like the bending energy. Therefore, unlike discs of K>0 [15], in hyperbolic discs there is an equipartition of bending and stretching energies.

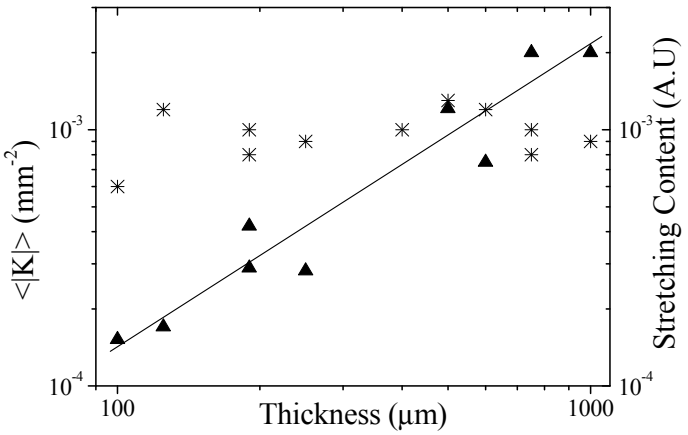

Figure 4: The average value of the Gaussian curvature (stars) is close to K_{tar} for all disc thickness indicating that on average all configurations are nearly stretch-free. Estimation of the stretching content by $\langle S \rangle \approx \frac{\langle \Delta K^2 \rangle}{n^4}$ (triangles) shows a linear (solid line) dependence on the initial thickness.

Using discs of constant target Gaussian curvature we have quantitatively measured and characterized two qualitatively different energy minimization strategies in non-Euclidean plates. Discs of $K_{tar} > 0$ minimize their energy via the scenario discussed in [16] i.e. by settling "near" the isometric embedding of g_{tar} , which is of lowest bending content, and smoothly approach it as the thickness decreases. As a result the only morphological changes are within their boundary layer, their bending content is bounded (by that of the selected embedding) and their bending energy decays like t_0^3. Hyperbolic discs, on the other hand, minimize their energy via a set of bifurcations that lead to refinement of wavy configurations (without necessarily forming multi-scale configurations as was observed previously). With decreasing thickness, their bending content increases roughly as t_0^{-1}, leading to slow decrease of their bending energy, $E_b \sim t_0^2$.Their stretching energy scales as t_0^2, as well, indicating an equipartition of stretching and bending energies.

The observed refinement is far from trivial. Different explicit constructions suggest that for finite surfaces of $K_{tar} = const < 0$ there exist exact embeddings with finite bending content[17],[18]. In this case one would expect the hyperbolic disc to behave similarly to the elliptic ones, i.e. via the scenario discussed in [16]. This is not what is found in our experiments. When considering the possible origin of this contradiction, one should remember that for every physical system, the accuracy of determining the target metric is finite. In our experiments the deviations of the imposed metric from the analytical expressions were below 2%. It well could be that for hyperbolic metrics

(and not for elliptic ones) there is an unusual sensitivity for "perturbations" to g_{tar}. We hope the results presented in this paper will motivate theoretical and numerical studies that will shed light on the observed behavior.

Acknowledgments This work was supported by the United States-Israel Binational Foundation (grant 2004037),the ERC SoftGrowth project and the NSF through award DMS-0807501.

References

1 E. Sharon, B. Roman, M. Marder, et al., *Nature* 419, 579 (2002).
2 E. Sharon, B. Roman, and H. L. Swinney, *Phys. Rev.* **E** 75 (2007).
3 Y. Klein, E. Efrati, and E. Sharon, *Science* 315, 1116 (2007).
4 U. Nath, B. C. W. Crawford, R. Carpenter, et al., *Science* 299, 1404 (2003).
5 B. O'neill, *Elementary Differential Geometry* (Academic Press, New York, 1997).
6 M. Marder and N. Papanicolaou, *Jour. Stat. Phys.* 125, 1069 (2006).
7 E. Efrati, Y. Klein, H. Aharoni, et al., *Physica D* 235, 29 (2007).
8 M. Marder, E. Sharon, S. Smith, et al., *Europhys Lett* 62, 498 (2003).
9 B. Audoly and A. Boudaoud, *Phys. Rev. Lett.* 91 (2003).
10 S. Nechaev and J. Voiturier, *Phys. A* 34, 11069 (2001).
11 J. Dervaux and M. Ben Amar, *Phys. Rev. Lett.* 101 (2008).
12 C. D. Santangelo, *Europhys Lett* 86 (2009).
13 E. Efrati, E. Sharon, and R. Kupferman, *Jour. Mech. Phys. Solids* 57, 762 (2009).
14 In general, K_{tar} itself is a function of the Lagrangian position on the sheet, while the surface measurements provide K in Eulerian coordinates. In such cases it is impossible to correctly calculate ΔK.
15 E. Efrati, E. Sharon, and R. Kupferman, *Phys. Rev.* **E** 80, 016602 (2009).
16 M. Lewicka and M. R. Pakzad, Preprint (2009).
17 E. Poznyak and E. Shikin, *Jour. Mat. Sci.* 74, 1078 (1995).
18 j. Gemmer and S. Venkataramani, arXiv:1005.4442v2 (2010).